



Pacific Northwest
NATIONAL LABORATORY

Proudly Operated by Battelle Since 1965

Maximum Potential Hydrogen Gas Retention in the sRF Resin Ion Exchange Column for the LAWPS Process

January 2018

PA Gauglitz
BE Wells
CLH Bottenus
PP Schonewill

DISCLAIMER

This report was prepared as an account of work sponsored by an agency of the United States Government. Neither the United States Government nor any agency thereof, nor Battelle Memorial Institute, nor any of their employees, makes **any warranty, express or implied, or assumes any legal liability or responsibility for the accuracy, completeness, or usefulness of any information, apparatus, product, or process disclosed, or represents that its use would not infringe privately owned rights.** Reference herein to any specific commercial product, process, or service by trade name, trademark, manufacturer, or otherwise does not necessarily constitute or imply its endorsement, recommendation, or favoring by the United States Government or any agency thereof, or Battelle Memorial Institute. The views and opinions of authors expressed herein do not necessarily state or reflect those of the United States Government or any agency thereof.

PACIFIC NORTHWEST NATIONAL LABORATORY
operated by
BATTELLE
for the
UNITED STATES DEPARTMENT OF ENERGY
under Contract DE-AC05-76RL01830

Printed in the United States of America

Available to DOE and DOE contractors from the
Office of Scientific and Technical Information,
P.O. Box 62, Oak Ridge, TN 37831-0062;
ph: (865) 576-8401
fax: (865) 576-5728
email: reports@adonis.osti.gov

Available to the public from the National Technical Information Service
5301 Shawnee Rd., Alexandria, VA 22312
ph: (800) 553-NTIS (6847)
email: orders@ntis.gov <<http://www.ntis.gov/about/form.aspx>>
Online ordering: <http://www.ntis.gov>



This document was printed on recycled paper.

(8/2010)

Maximum Potential Hydrogen Gas Retention in the sRF Resin Ion Exchange Column for the LAWPS Process

PA Gauglitz
BE Wells
CLH Bottenus
PP Schonewill

January 2018

Prepared for
the U.S. Department of Energy
under Contract DE-AC05-76RL01830

Pacific Northwest National Laboratory
Richland, Washington 99352

Executive Summary

The Low-Activity Waste Pretreatment System (LAWPS) is being developed to provide treated supernatant liquid from the Hanford tank farms directly to the Low-Activity Waste (LAW) Vitrification Facility at the Hanford Tank Waste Treatment and Immobilization Plant. The design and development of the LAWPS is being conducted by Washington River Protection Solutions, LLC. A key process in LAWPS is the removal of radioactive Cs in ion exchange (IX) columns filled with spherical resorcinol-formaldehyde (sRF) resin. One accident scenario being evaluated is the loss of liquid flow through the sRF resin bed after it has been loaded with radioactive Cs and hydrogen gas is being generated by radiolysis. In normal operations, the generated hydrogen is expected to remain dissolved in the liquid and be continuously removed by liquid flow. For an accident scenario with a loss of flow, hydrogen gas can be retained within the IX column both in the sRF resin and below the bottom screen that supports the resin within the column. The purpose of this report is to summarize calculations that estimate the upper-bound volume of hydrogen gas that can be retained in the column and potentially be released to the headspace of the IX column or to process equipment connected to the IX column and, thus, pose a flammability hazard.

An evaluation of gas retention mechanisms shows that hydrogen bubbles are expected to be retained in the bed of sRF resin. The largest retained hydrogen volume in the sRF resin bed occurs when the settled bed of sRF resin becomes neutrally buoyant in the supernatant liquid. Once gas retention causes the sRF resin bed to exceed neutral buoyancy, a spontaneous gas release event is expected that has the potential to release all of the hydrogen gas retained in the bed. In addition to hydrogen retention in the settled bed of sRF resin, hydrogen gas is also expected to be retained below the Johnson screen that supports the sRF resin within the column; this is due to surface tension and the resulting capillary pressure that resists the ability of a gas bubble to penetrate the Johnson screen and/or the bed of sRF particles supported by the screen.

The location of the retained gas and the height of liquid above it affect the pressure of the gas and its volume when released from the column to atmospheric pressure. Three cases are considered for the location and quantity of retained gas, and for each case, results are given for two different gas retention mechanisms and three different fluids. These cases and conditions were selected to provide bounding (maximum) estimates of the gas volume released. The largest gas volume released occurs with water in the column in comparison to a liquid having nominal LAW physical properties and to a liquid having the bounding high density for LAW. Further, the largest gas volume released occurs using the neutral buoyant gas fraction with gas retained in liquid-displacing bubbles rather than by the alternate particle-displacing bubble gas retention mechanism. The maximum calculated volume of released gas is 0.521 m³ at 1 atm pressure and 20 °C or, equivalently, 21.6 moles, which was determined assuming gas retention at a conservatively-low column temperature of 20 °C and a pre-gas-retention liquid depth of 2.13 m (84 in.) above the bottom screen. The volume of gas released increases by approximately 9% for a nominally 50% increase in pre-gas-retention liquid depth in the system from 2.13 m to 3.18 m (125 in.).

Acknowledgements

The authors would like to thank Lenna Mahoney for her review of some of the calculations and Scot Rassat for his overall review of the report and the resulting improvement in technical clarity. We would also like to thank Bill Dey for his guidance on quality assurance matters and Matt Wilburn for his helpful editing.

Acronyms and Abbreviations

IX	ion exchange
LAW	low-activity waste
LAWPS	Low-Activity Waste Pretreatment System
PNNL	Pacific Northwest National Laboratory
QA	quality assurance
R&D	research and development
sRF	spherical resorcinol-formaldehyde
WRPS	Washington River Protection Solutions, LLC
WWFTP	WRPS Waste Form Testing Program

Nomenclature

α_{NB}	gas void fraction at neutral buoyancy in a settled bed for particle-displacing bubbles
$\alpha_{NB,LD}$	gas void fraction at neutral buoyancy in a settled bed with interstitial-liquid-displacing bubbles
ΔP	pressure difference between gas and liquid across a curved interface
$\Delta \rho$	density difference between gas and liquid
θ	contact angle of gas advancing on Vee-Wire [®] of Johnson screen
σ	surface tension of the gas bubble/liquid interface
φ	angle of Vee-Wire [®] on Johnson screen
ϕ_b	sRF resin bed porosity
ρ_L	liquid layer density
ρ_P	resin bead (particle) density
ρ_S	gas-free sediment layer density
d	width of slot for Johnson screen
g	gravitational acceleration
h	height of pancake bubble
H_b	sRF resin bed height
H_L	supernatant liquid layer height
P_A	atmospheric pressure
P_c	capillary entry pressure
\hat{P}_c	normalized capillary entry pressure
P_{gas}	pressure in gas bubbles (with hydrostatic head)
R	length in Figure 4.2

R_1, R_2 radii of curvature for gas/liquid interface
 R_B radius of spherical bead
 R_m radius of circle for pore throat between close-packed beads

Contents

Executive Summary	iii
Acknowledgements	iv
Acronyms and Abbreviations	v
Nomenclature	v
1.0 Introduction	1.1
1.1 Gas Retention Scenarios in the IX Column	1.3
2.0 Quality Assurance	2.1
3.0 sRF Resin Column Configuration and Fluid and sRF Resin Properties	3.1
4.0 Potential Pancake Bubble below the Bottom Screen	4.1
5.0 Potential Retained Gas Volume in sRF Resin Bed Released to Break Tank	5.1
5.1 Calculation Method	5.1
5.1.1 Resin Bed Retained Gas Volume	5.1
5.1.2 Large Bubble Retained Gas Volume	5.2
5.1.3 Release Volume into Break Tank	5.2
5.2 Results	5.3
6.0 Conclusions	6.1
7.0 References	7.1

Figures

Figure 1.1. Planned full-scale sRF resin IX bed and conceptual configuration of break tank for removal of flammable gases with resin bed fluidization (Aguilar 2016). Note that the recirculation pump and the resin bed fluidization capability depicted in Figure 1.1 are not applied in this analysis.....	1.2
Figure 1.2. Simplified configuration of retained gas in IX column.	1.3
Figure 1.3. Two mechanisms of bubble retention in packed beds of particles: Interstitial-liquid-displacing and particle-displacing bubbles.	1.4
Figure 1.4. Top-view of a Vee-Wire® Johnson screen and side-view of gas necking through the slots in the screen.	1.5
Figure 1.5. Gas necking through the openings between sRF resin beads supported on the Johnson (Vee-Wire®) screen.....	1.5
Figure 4.1. Configuration of a gas bubble entering the slot of a Johnson screen where R_1 is the radius of curvature, h is the height of the gas bubble, d is the width of the slots in the screen, θ is the contact angle and, φ is the angle of incline of the Vee-Wire®.....	4.2
Figure 4.2. Geometry of a non-wetting gas phase in the pore throat between uniform, hexagonally close-packed spheres (Kruyer 1958).	4.4
Figure 5.1. Release volume for Table 5.2 limiting cases as a function of height of liquid column above Johnson screen.....	5.5

Tables

Table 3.1. Dimensions of the IX Column, sRF Resin Bed, and Johnson Screen.....	3.1
Table 3.2. Liquid and sRF Resin Particle and Bed Properties	3.2
Table 4.1. Pancake Bubble Height Based on Capillary Entry Pressure of the Bottom Screen for Different Liquids.....	4.2
Table 4.2. Range of Normalized Capillary Entry Pressures Based on Experimental Data and Comparison to Theoretical Limit.....	4.4
Table 4.3. Pancake Bubble Height Based on Capillary Entry Pressure of the sRF Resin for Different Liquid/sRF Resin Systems	4.5
Table 5.1. Results for Cases 1 through 3, Particle-Displacing Bubbles.....	5.4
Table 5.2. Results for Cases 1 through 3, Liquid-Displacing Bubbles	5.4

1.0 Introduction

The primary mission of the U.S. Department of Energy Office of River Protection is to retrieve and process approximately 56 million gallons of radioactive waste from 177 underground tanks located on the Hanford Site. As part of achieving this mission, Washington River Protection Solutions, LLC (WRPS) is developing the Low-Activity Waste Pretreatment System (LAWPS) to provide treated supernatant liquid from the Hanford tank farms directly to the Low-Activity Waste (LAW) Vitrification Facility at the Hanford Tank Waste Treatment and Immobilization Plant (Ansolabehere 2016).

A key process in LAWPS is the removal of radioactive Cs using columns filled with spherical resorcinol-formaldehyde (sRF) ion exchange (IX) resin (Ansolabehere 2016; Aguilar 2016). One accident scenario being evaluated for this process is the loss of liquid flow through the sRF resin bed after it has been loaded with radioactive Cs and hydrogen gas is being generated by radiolysis. In normal operations with liquid flow, the generated hydrogen is expected to remain dissolved in the liquid and be continuously removed by liquid flow. For an accident scenario with a loss of liquid flow, hydrogen gas can be retained within the IX column both in the sRF resin and below the bottom screen that supports the resin within the column. The objective of this study is to estimate an upper-bound volume of hydrogen gas that can be retained in the column and potentially be released to the headspace of the IX column or to process equipment connected to the IX column and, thus, pose a flammability hazard.

Figure 1.1 shows a general schematic of the planned full-scale sRF resin IX bed and the conceptual configuration of a break tank for removal of hydrogen gas that might be released from the IX column (Aguilar 2016). The dimensions shown in Figure 1.1 will be used for estimating the maximum potential volume of retained hydrogen gas that can be released to the break tank that is ventilated with air, and these dimensions are summarized in Section 3.0. Note that the recirculation pump and the resin bed fluidization capability depicted in Figure 1.1 are not applied in this analysis.

The approach for estimating the maximum potential retained hydrogen gas is to postulate likely scenarios for the location and mechanisms of retaining hydrogen bubbles in the IX column, based on the existing understanding of gas retention mechanisms, and then calculate the amount of hydrogen retained for each scenario to determine the bounding conditions. Because the location of the retained gas affects the volume of hydrogen when released, due to the difference in hydrostatic head from the top to the bottom of the column, the technical approach includes estimating the volume of gas after it has been released into the break tank at ambient pressure.

Section 1.1 summarizes the expected mechanisms of gas bubble retention in the sRF resin and below the bottom screen in the IX column and describes three scenarios for maximum retention in the IX column. Following a discussion in Section 2.0 of the quality assurance (QA) program and requirements, Section 3.0 summarizes the IX column configuration and fluid and sRF resin properties. Section 4.0 gives the technical approach and results for the potential size of a pancake bubble below the bottom screen, and Section 5.0 provides the calculation approach and results for the maximum potential volume of hydrogen gas for the combination of gas retention in the sRF resin bed and in a pancake bubble for the three scenarios.

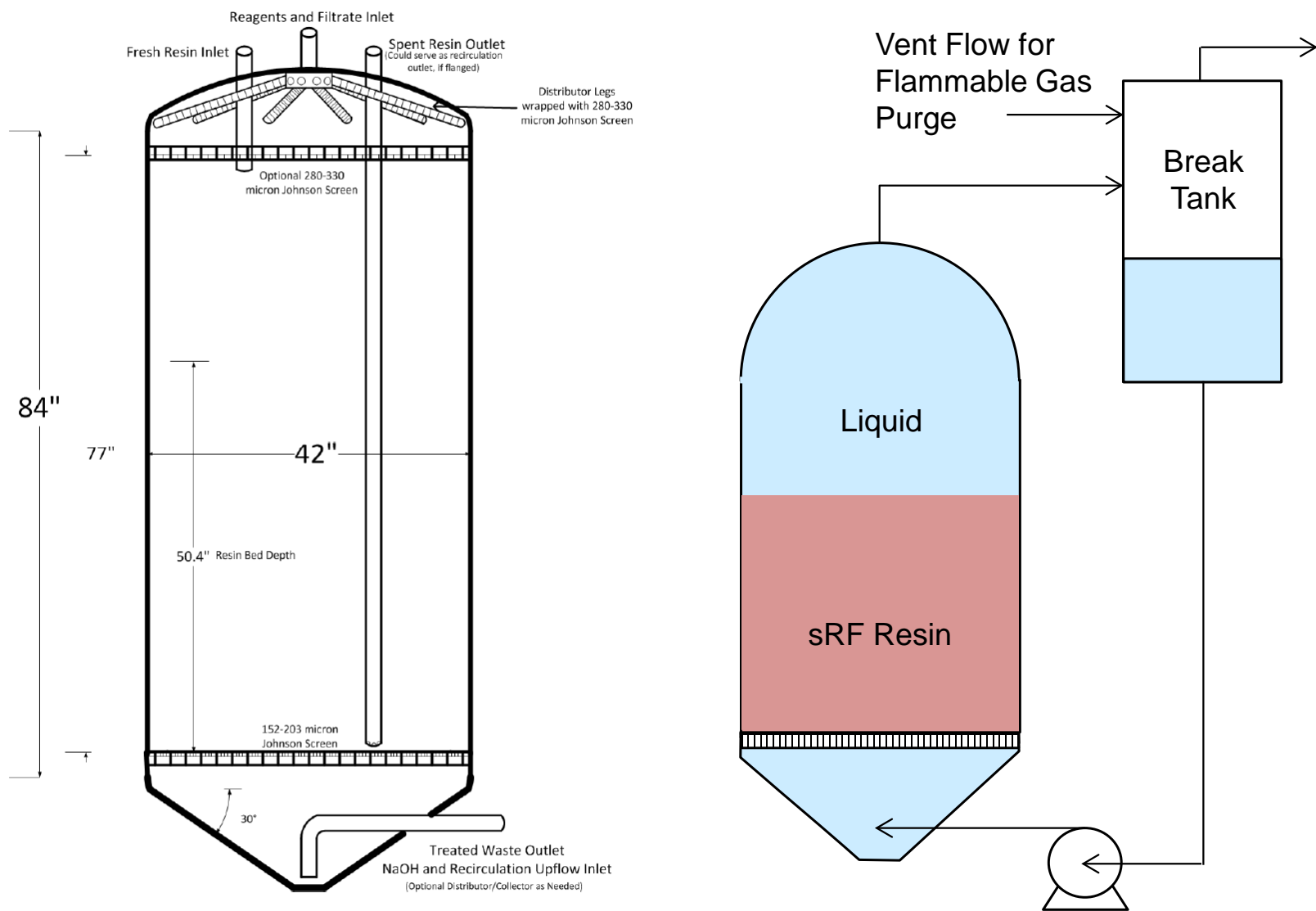


Figure 1.1. Planned full-scale sRF resin IX bed and conceptual configuration of break tank for removal of flammable gases with resin bed fluidization (Aguilar 2016). Note that the recirculation pump and the resin bed fluidization capability depicted in Figure 1.1 are not applied in this analysis.

1.1 Gas Retention Scenarios in the IX Column

When hydrogen (H_2) is being generated by radiolysis within an IX column and is not removed by flowing liquid, individual gas bubbles can form and are expected to be retained in the settled bed of sRF resin. It is also possible for a large and flat “pancake” bubble to be retained below the bottom screen. Figure 1.2 shows a simplified configuration of the IX column and the location of retained gas that will be used for estimating the maximum potential volume of gas that can be retained in the IX column. Figure 1.2 also shows how the level of the sRF resin bed and the liquid level can increase. The location of the retained gas and the height of the liquid level are important for determining the hydrostatic pressure on the bubbles and the volume expansion when the gas is released from the column. A more accurate configuration of the column would include a non-cylindrical region below the bottom screen (the simplified configuration conservatively overestimates the volume of gas in the pancake bubble) and the upper region of the column would also be non-cylindrical and connected with piping that might increase the hydrostatic head on the retained bubbles. The effect of increasing the hydrostatic head, presumably due to liquid in piping above the column, is included in the analysis of the maximum retained gas.

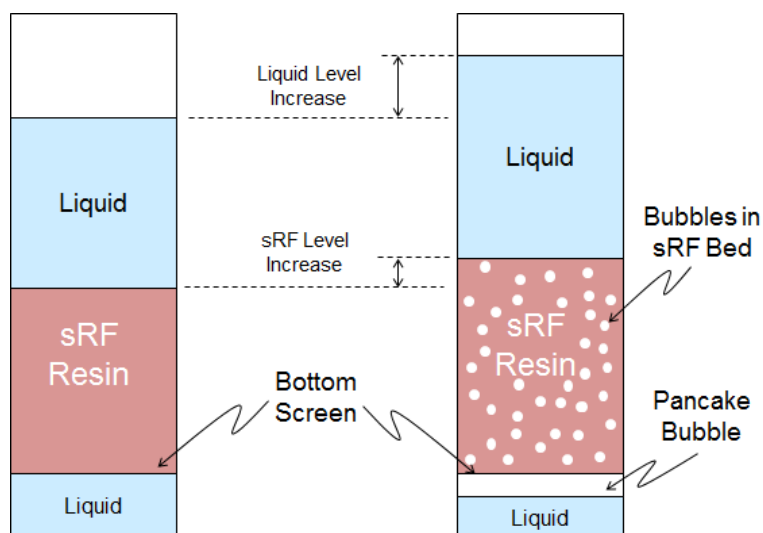


Figure 1.2. Simplified configuration of retained gas in IX column.

Bubble retention in settled beds of particles has been studied previously, and Gauglitz et al. (2012) and Schonewill et al. (2014) provide reviews of these studies. One key observation was that different mechanisms of gas retention will occur depending on the size of the settled particles, the bed height, and fluid and particle densities. Figure 1.3 shows interstitial-liquid-displacing and particle-displacing bubbles retained within packed beds of particles (Gauglitz et al. 2012). Both of these gas retention mechanisms can occur in a bed of sRF resin, and they affect the settled bed differently. Because the hydrostatic head on the bubbles changes the volume of gas when released from the column, there is a need to describe how the different retention mechanisms affect the liquid and sRF resin levels in the column. For interstitial-liquid-displacing bubbles, liquid is expelled from the bed, causing a rise in liquid level, but the sRF resin bed itself does not expand. In contrast, particle-displacing bubbles displace both particles and liquid, and this causes expansion of the sRF resin bed together with a rise in liquid level. To simplify and bound the estimate of maximum retained gas volume, separate analyses are conducted using only particle-displacing

bubbles and only interstitial-liquid-displacing bubbles, although both bubble types are likely to be present in the actual system.

As the volume of retained gas increases, a point is reached at which a spontaneous gas release occurs. The retained volume is at a maximum just prior to the spontaneous release. For beds of settled particles below a supernatant liquid layer, a buoyant displacement gas release event will occur when a settled bed with retained gas is neutrally buoyant in the supernatant liquid (Meyer et al. 1997). This represents the maximum potential retained gas volume within the resin bed.¹

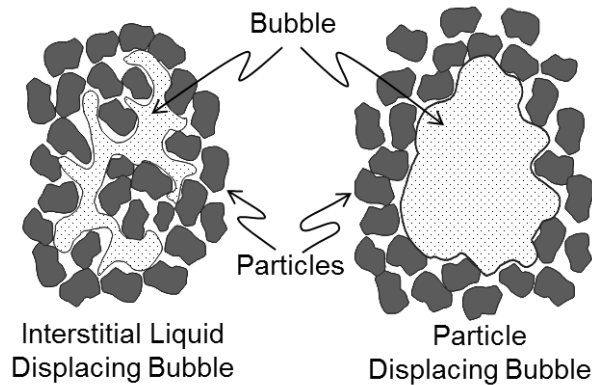


Figure 1.3. Two mechanisms of bubble retention in packed beds of particles: Interstitial-liquid-displacing and particle-displacing bubbles.

The bottom screen, as indicated in Figure 1.1, is intended to be a Johnson screen (Johnson Screens, Aqseptence Group, Inc., New Brighton, MN), which is composed of vee-shaped wires (Vee-Wire[®]) supported by rods with uniform slots between the wires. Figure 1.4 shows a typical configuration of a Johnson screen. Figure 1.4 also shows the configuration of gas as it necks into the slots between the wires from below the screen, forming multiple individual bubble fronts. The surface tension between the gas and liquid causes a pressure difference across the curved gas/liquid interface that is often called the capillary pressure (Dullien 1992). For the front of a gas bubble to penetrate through the slot, the gas pressure needs to exceed the liquid pressure by the capillary pressure, and the magnitude of the capillary pressure increases as the opening becomes smaller. At the narrowest point in an opening, the capillary pressure reaches a maximum, often called the capillary entry pressure. Because of surface tension and the resulting capillary entry pressure, a large bubble can easily be held below the bottom screen. Section 4.0 provides an estimate for the maximum height of a pancake bubble retained below a slotted screen.

¹ If a settled layer has strength, somewhat more buoyancy is needed to initiate a gas release event. Based on informal (For Information Only) visual observations of sRF resin particles in liquids, they behave as non-cohesive (non-sticky) particles, and a settled bed of sRF resin is not expected to need additional buoyancy to initiate gas release.

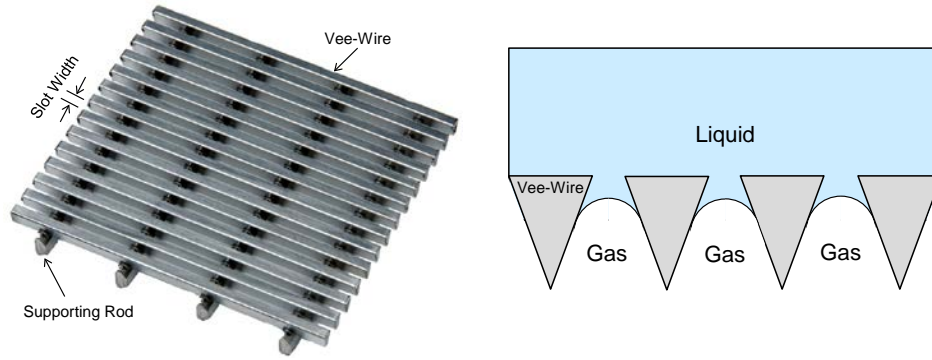


Figure 1.4. Top-view of a Vee-Wire[®] Johnson screen and side-view of gas necking through the slots in the screen.

Figure 1.5 shows a configuration of gas (bubble fronts) necking through the openings between sRF resin beads that are supported by a Vee-Wire[®] screen. In this configuration, the openings between the sRF beads are smaller than the slots in the screen. For this configuration, the height of a potential bubble below the screen is greater than that of a bubble held by the slots in the screen. Section 4.0 provides an estimate for the maximum height of a pancake bubble held by a settled bed of sRF resin beads.

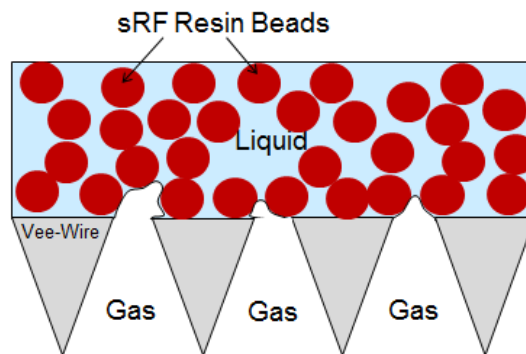


Figure 1.5. Gas necking through the openings between sRF resin beads supported on the Johnson (Vee-Wire[®]) screen.

As discussed above, hydrogen gas can be retained both in a settled bed of sRF resin and in a pancake bubble that forms under, and as a result, the Johnson screen that supports the resin and/or the pore throats of the resin bed. Three different gas retention scenarios (cases) are considered for determining the maximum potential volume of gas released from the column.

- Case 1 – The sRF resin bed retains gas to be neutrally buoyant, and the maximum potential pancake bubble based on the slot opening in the Johnson screen also being retained. While it is unlikely that gas within the sRF resin bed and the gas below the Johnson screen would simultaneously reach their individual maximum retention values, this is a reasonable upper bound. This configuration is also physically plausible, but experiments have not been conducted to confirm this.
- Case 2 – The volume of uniformly distributed gas needed to make the sRF resin bed neutrally buoyant is first determined, and this volume of gas is then placed below the bottom screen to maximize the hydrostatic head and thus maximize the gas volume when released from the column. The volume of gas below the bottom screen is only the amount needed to make the sRF resin bed neutrally buoyant (i.e., no additional pancake bubble volume is considered), and it is assumed that no

gas is retained in the resin bed. This is a hypothetical configuration, but it is useful for estimating the maximum retained gas volume. If a bottom screen design is used that eliminates retention by the screen, this case represents the maximum volume of gas when released based on neutral buoyancy in the sRF resin bed.

- Case 3 – The sRF resin bed retains gas to be neutrally buoyant, and the maximum potential pancake bubble based on the pore throats in the sRF resin bed is also retained below the bottom of the bed (and the screen). This is an unphysical, but worst-case, bounding limit for gas retention in the column. The case is not physically plausible due to the fact that a neutrally buoyant sRF resin bed cannot support an additional gas volume in a pancake bubble, because the sRF resin bed would be displaced upward and release gas if a pancake bubble attempted to enter the bed from below. Further, for a pancake bubble that passes through the bottom screen, but does not enter the resin bed due to restriction by pore throats, the maximum volume (and equivalent height) of the pancake bubble is that which makes the resin bed, including any gas retained within, neutrally buoyant. This is bounded by Cases 1 and 2.

For each of these scenarios, gas release volumes are calculated for both particle-displacing and interstitial-liquid-displacing bubble retention mechanisms and for three different fluids equilibrated with sRF resin. The gas release volumes for these eighteen conditions (3 Cases \times 2 bubble retention mechanisms \times 3 fluids), from which the bounding (maximum gas volume released) condition is determined, are summarized in Section 5.0.

2.0 Quality Assurance

This work was conducted with funding from WRPS under contract 36437-187, “*LAWPS Integrated Support Testing*,” *Low-Activity Waste Pretreatment System (LAWPS) Integrated Testing Project*. The work was conducted as part of Pacific Northwest National Laboratory (PNNL) project 67535.

All research and development (R&D) work at PNNL is performed in accordance with PNNL’s Laboratory-Level Quality Management Program, which is based on a graded application of NQA-1-2000, *Quality Assurance Requirements for Nuclear Facility Applications*, to R&D activities. To ensure that all client QA expectations were addressed, the QA controls of the WRPS Waste Form Testing Program (WWFTP) QA program were also implemented for this work. The WWFTP QA program implements the requirements of NQA-1-2008, *Quality Assurance Requirements for Nuclear Facility Applications*, and NQA-1a-2009, *Addenda to ASME NQA-1–2008*, and consists of the WWFTP *Quality Assurance Plan* (QA-WWFTP-001) and associated QA-NSLW-numbered procedures that provide detailed instructions for implementing NQA-1 requirements for R&D work.

Specific details of this project’s approach to assuring quality are contained in the *LAWPS Testing Program Quality Assurance Plan* (67535-QA-001, Rev. 0) and associated implementing procedures. The QA plan describes how the procedures of the WWFTP QA program were used in conducting the work. The work described in this report was assigned the technology level “Applied Research,” and was planned, performed, documented, and reported in accordance with procedure QA-NSLW-1102, *Scientific Investigation for Applied Research*. All staff members contributing to the work received proper technical and QA training prior to performing quality-affecting work.

3.0 sRF Resin Column Configuration and Fluid and sRF Resin Properties

To estimate the volumes of retained and potentially released gas, a number of physical properties and dimensions are needed. For the column, dimensions are needed for the depth of the gas-free sRF resin bed and the total depth of fluid in the column. The slot width of the Johnson screen is also needed for estimating the height of a gas bubble needed to overcome the capillary entry pressure that resists the penetration of a pancake bubble through the screen. Table 3.1 summarizes these dimensions.

Table 3.1. Dimensions of the IX Column, sRF Resin Bed, and Johnson Screen

	Dimension ^(a)	
Height of sRF Resin Bed (Gas-Free)	1.28 m	50.4 in.
Total Liquid Depth	2.13 m	84 in. ^(b)
IX Column Diameter	1.07 m	42 in.
Bottom Johnson Screen Slot Width	152 μm	-

(a) Dimension taken from Figure 1.1, which is reproduced from Figure 3-3 of Aguilar 2016. The minimum slot width identified in Figure 1.1 was selected because it maximizes the height of a potential pancake bubble.

(b) In Figure 1.1, this value represents the height from a few inches below the Johnson screen to approximately the bottom of the distributor legs at the top of the column. This height is used as an estimate for the total liquid depth, which neglects any liquid depth in piping above the column. (In Section 5.0, the effect of a nominally 50% increase in liquid depth on gas release is evaluated.)

To determine maximum gas retention in the sRF resin bed (neutral buoyancy of the bed in the supernatant liquid), which is presented in Section 5.0, the densities of the supernatant liquid and sRF resin beads (particles) and the porosity of the settled sRF resin bed are needed. To determine the maximum volume of a pancake bubble, which is presented in Section 4.0, the surface tension of the gas/liquid interface and the sRF particle diameter are also needed. The sRF particles are unique in that they are porous particles that change density and size depending on 1) the density and chemical constituents of the suspending solution in which they are equilibrated, and 2) whether the particles have been contacted with NaOH and are in the Na⁺ form or if they have been contacted with acid, such as HNO₃, and are in the H⁺ form. Table 3.2 summarizes these parameter values for the different sRF particle conditions and liquids used in analyses.

Liquid densities were measured with a pycnometer and the sRF particle density was measured with a displacement method (Flint and Flint 2002). For the displacement method, the liquid density is independently determined using a pycnometer; separately, a measured mass of sRF particles is added to a pycnometer that is then filled with the suspending liquid and re-weighed. From the liquid density and mass measurements, the volume and density of the sRF particles can be determined. The sRF particles are porous and contain the suspending liquid within the particles. For these measurements, particles equilibrated with a suspending fluid were removed from the liquid and hand-dried by blotting with absorbent paper until the surface moisture was removed but the particles still contained the internal liquid.

The sRF particle diameters shown in Table 3.2 were determined from optical microscopy photographs using a calibrated micro-ruler and are the average of 20 particles. Further details of the density and diameter measurements will be summarized in a future report.¹

Table 3.2. Liquid and sRF Resin Particle and Bed Properties

Supernatant / Resin Form	Temp (°C)	Liquid Density (kg/m ³)	sRF Particle Density (kg/m ³)	sRF Particle Diameter (µm)	Surface Tension (mN/m)	Gas-Free sRF Bed Porosity (%)
Hot Water	70 ^(a)	977.8 ^(c)	N/A	N/A	64 ^(c)	35.9 ^(h)
Ambient Water / Na ⁺	Ambient ^(b)	998.4	1,224	439	72 ^(f)	35.9 ^(h)
Ambient Water / H ⁺	Ambient ^(b)	996.8	1,190	414	72 ^(f)	35.9 ^(h)
Nominal LAW / Na ⁺	Ambient ^(b)	1,231	1,367	455	85 ^(g)	35.9 ^(h)
High-Limit LAW / Na ⁺	Ambient	1,350 ^(d)	1,443 ^(e)	463 ^(e)	100 ^(d)	35.9 ^(h)

- (a) This is the highest temperature used in gas generation studies with sRF resin (Colburn et al. 2017) and is selected as the maximum temperature for this analysis.
- (b) Ambient temperature measurements were taken between 21 and 23 °C.
- (c) CRC 2005
- (d) Ansolabehere 2016, Table 3-3 (upper limit of range)
- (e) Based on linear extrapolation of measured Na⁺-form sRF resin and liquid densities and particle diameters in water and Nominal LAW.
- (f) CRC 2005 at 25 °C (25 °C was selected as a representative ambient temperature; 20 °C would give a higher value of 73 mN/m, but this value would not change the bounding pancake bubbles heights in Table 4.1 and Table 4.3.)
- (g) Extrapolation to 20 °C of results from 30 to 60 °C in Norton and Pederson 1994, Fig. 19, for simulant SY1-SIM-93B with no added ammonia.
- (h) Minimum porosity given by Dullien (1992), Section 1.2.8.2, for “close random packing” of identical spheres. The minimum porosity for this range was selected because a lower porosity gives a high-density sRF resin bed and a higher neutral-buoyancy gas fraction (see Section 5.1.1) and, accordingly, provides a higher (conservative) volume of retained gas.

N/A = not applicable

¹ The methods for measuring sRF particle and liquid densities by the displacement method and particle diameters from microscope images will be described more completely in a future report: *Gas Retention, Gas Release, and Fluidization of Spherical Resorcinol-Formaldehyde (sRF) Ion Exchange Resin*, RPT-LPIST-005.

4.0 Potential Pancake Bubble below the Bottom Screen

A gas bubble can be retained below the bottom screen due to surface tension forces, or capillary forces, resisting the entry of the gas bubble through the narrow slots in the screen or the narrow pore throats in a settled sRF resin bed. A sufficiently large bubble may span the entire cross-section below the bottom screen and can be described as a pancake bubble. For pore throats with simple shapes, the pressure difference needed for a non-wetting phase, such as an air bubble, to pass through a pore throat filled with a wetting liquid, such as water, can be determined from the Young-Laplace equation (Dullien 1992). Eq. (4.1) gives the Young-Laplace equation for the pressure difference across a curved interface between two static fluids due to surface tension and the shape of the interface:

$$\Delta P = P_c = \sigma \left(\frac{1}{R_1} + \frac{1}{R_2} \right) \quad (4.1)$$

where ΔP is the pressure difference, σ is the surface tension of the liquid, and R_1 and R_2 are the orthogonal radii of curvature. The pressure difference given by Eq. (4.1) is often called the capillary pressure, P_c , and when the pressure difference is sufficient for a gas bubble to enter a pore throat it is called the capillary entry pressure (Dullien 1992). For the more complicated shapes of bubbles entering pore throats in porous materials, such as random packs of spheres, the capillary entry pressure can be estimated with the Young-Laplace equation, but typically using idealized pore geometries. An alternate approach for porous materials is to use experimental measurements of the fraction of the pore volume occupied by a non-wetting (gas) phase as a function of the applied capillary pressure, and estimating a capillary entry pressure from this relationship.

In equilibrium, and with continuous gas and liquid phases, the capillary pressure is balanced by hydrostatic pressure, and this gives a relationship between the capillary pressure and the height of a pancake bubble:

$$P_c = \Delta \rho g h \quad (4.2)$$

where $\Delta \rho$ is the difference in density between the two immiscible fluids, g is gravitational acceleration, and h is the height or thickness of a bubble. Below, the capillary entry pressure for the Johnson screen and corresponding potential pancake bubble height will be determined first and then the same will be estimated for a settled bed of sRF resin.

Figure 4.1 shows the geometry of a bubble front entering into the slot between the wires of a Johnson screen and a corresponding pancake bubble of height h in a column. For the slots in the Johnson screen, the bubble front has a cylindrical shape with $R_1 \ll R_2$. Assuming the contact angle is zero, which gives the largest capillary entry pressure and pancake bubble height, Eq. (4.1) simplifies to

$$P_c = \sigma \left(\frac{1}{R_1} \right) \quad (4.3)$$

The largest capillary entry pressure occurs when the bubble front is at the narrowest opening of the slot where the side of the bubble is at the sharp corners of the vee wires and $R_1 = d/2$. When the bubble is at this location, R_1 does not depend on angle of incline of the Vee-Wire®. Combining and re-arranging

Eqs. (4.2) and (4.3), gives the following relationship for the pancake bubble height:

$$h = \frac{\sigma}{\Delta\rho g} \left(\frac{1}{R_1} \right) \quad (4.4)$$

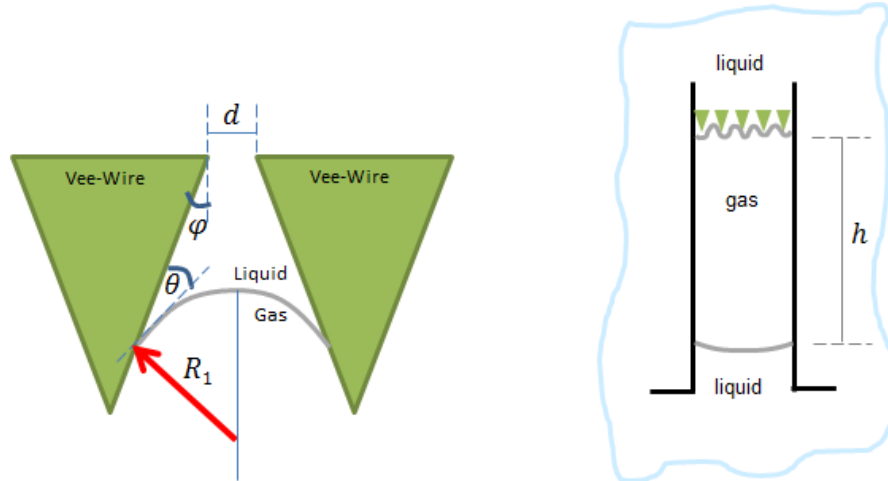


Figure 4.1. Configuration of a gas bubble entering the slot of a Johnson screen where R_1 is the radius of curvature, h is the height of the gas bubble, d is the width of the slots in the screen, θ is the contact angle and, ϕ is the angle of incline of the Vee-Wire®.

Table 4.1 gives results for the pancake bubble height for the bottom screen using the slot width given in Table 3.1 ($R_1 = d/2$), the fluid properties given in Table 3.2, and assuming a negligible gas density for the density difference $\Delta\rho$. As shown by Eq.(4.4), the pancake bubble height increases with increasing surface tension but decreases with increasing density difference. The high-limit LAW has the largest surface tension, and this fluid is predicted to have the tallest pancake bubble despite having the highest liquid density. The bottom screen has a well-defined geometry and the fluid properties for the high-limit LAW are also well-defined, so a bounding value of 10 cm (0.1 m), just slightly larger than the high-limit LAW value, is selected to be used in the Case 1 gas volume calculations in Section 5.0.

Table 4.1. Pancake Bubble Height Based on Capillary Entry Pressure of the Bottom Screen for Different Liquids

Fluid	h (cm)
Hot Water	8.8
Ambient Water / Na ⁺	9.7
Ambient Water / H ⁺	9.7
Nominal LAW / Na ⁺	9.3
High-Limit LAW / Na ⁺	9.9
Bounding Value for Maximum Gas Volume Estimates (Section 5.0)	10.0 ^(a)

(a) This value exceeds the highest calculated result for the high-limit LAW. Because the screen geometry and fluid properties are reasonably well-defined, the bounding value is essentially equal to the maximum calculated value.

For bubble entry through the pore throats between sRF resin particles, the capillary entry pressure is estimated using both an idealized pore geometry and experimental capillary entry pressure data for a number of literature studies using uniform diameter spherical beads. To compare the different estimates, a normalized capillary entry pressure, \hat{P}_c , as defined below, is used.

$$\hat{P}_c = \frac{P_c}{\sigma/R_B} \quad (4.5)$$

where R_B is the radius of the spherical beads. In the literature studies, the liquid and gas phases are, typically, water in air or mercury in air.

For potential idealized pore shapes, the geometry giving the highest capillary entry pressure is used, as this gives a bounding upper estimate for the height of a pancake bubble. The pore throat in hexagonally close-packed uniform spheres is the smallest potential throat and results in the largest capillary entry pressure. Figure 4.2 shows the geometry of the pore throat as an inscribed circle touching the spherical beads. As described by Kruyer (1958), and as shown in Figure 4.2, a geometrical relationship gives the radius of the pore throat between the close-packed spheres, R_m , in terms of the radius of the spherical beads as follows:

$$\cos(30^\circ) = \frac{R_B}{R_B + R_m} \quad (4.6)$$

Rearranging gives

$$\frac{R_B}{R_m} = \frac{\cos(30^\circ)}{1 - \cos(30^\circ)} = 6.464 \quad (4.7)$$

This result applies for uniformly-sized spherical beads of any radius. For a gas bubble with a hemispherical front entering this throat, the two radii of curvature in Eq. (4.1) (R_1 and R_2) are both equal to R_m . Combining this with Eq. (4.7), the normalized capillary entry pressure given by Eq. (4.5) becomes

$$\hat{P}_c = 2 \frac{R_B}{R_m} = 12.93 \quad (4.8)$$

This result is an upper bounding theoretical estimate for the capillary entry pressure of a uniform packing of sRF resin beads.

A number of experimental studies of porous materials have measured the fraction of the pore space occupied by a non-wetting phase as a function of the applied capillary pressure. As the capillary pressure is increased, the non-wetting phase enters progressively more of the pores as it displaces the wetting phase (air displacing water or mercury displacing air). There are a number of definitions in the literature for the capillary pressure of a non-wetting phase entering porous media. Dullien (1992) defines the breakthrough capillary pressure as corresponding to the “incipient formation of a continuum of the non-wetting phase through a pore network of arbitrarily large size,” which is a condition where the non-wetting phase can flow through the connected pore network. For this evaluation of literature data, this definition is used and the satisfying condition is approximated as the capillary pressure when the non-wetting phase occupied about 30 percent of the pore space. For simplicity in this report, this is called the

capillary entry pressure. This method of estimating the breakthrough capillary pressure was selected to overestimate the maximum height of a pancake bubble.

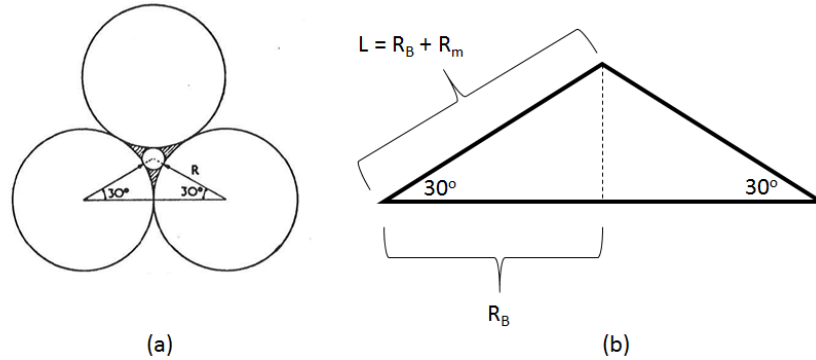


Figure 4.2. Geometry of a non-wetting gas phase in the pore throat between uniform, hexagonally close-packed spheres (Kruger 1958).

Table 4.2 summarizes experimental results from the literature, presented as normalized capillary entry pressures, and also shows the theoretical bounding estimate given by Eq. (4.8). There is variability in the literature values, but they are all noticeably less than the theoretical limit for hexagonal close-pack spheres. Because there are multiple experimental studies in the literature for packed beds of uniform spheres, which adequately represent settled beds of uniform sRF resin beads, and the literature results for the experimentally-based normalized capillary entry pressures are all considerably lower than the theoretical value, the experimental values can be used as a basis to estimate an upper bound for the capillary entry pressure in a bed of sRF resin. From the experimental results shown in Table 4.2, a normalized capillary entry pressure of 6.8 is the largest value, and this will be used for estimating the maximum height of a potential pancake bubble.

Table 4.2. Range of Normalized Capillary Entry Pressures Based on Experimental Data and Comparison to Theoretical Limit

Reference	Notes on Experimental Conditions	\hat{P}_c
Morrow and Harris 1965 (Fig. 4, pg. 21)	Glass beads (diameter 0.25-0.297 mm) Air displacing water R_B (average) 0.137 mm	4.9
Falls et al. (1988) (Table 1, pg. 887)	Multiple sets of uniform glass beads Air displacing water R_B 0.175 mm, 0.30 mm, and 0.40 mm	6.1
Dullien 1979 (Fig. 2.22, pg. 33)	Already given as \hat{P}_c	6.8 ^(a)
Dullien 1992 (Fig. 2.39, pg.175)	Glass beads (diameter 0.42-0.35 mm) Mercury displacing air	3.9
Originally presented by Kruger (1958) (Fig. 4, pg. 1763)	R_B (average) 0.193 mm	
Kruger 1958 (Table 2, pg. 1761)	Hexagonal close-packed (theoretical)	12.93

(a) Largest experimental value for the normalized capillary entry pressure

Using Eq.(4.2) together with the normalized capillary entry pressure definition in Eq. (4.5) gives the following relationship for maximum pancake bubble height based on the capillary entry pressure of the sRF resin.

$$h = \frac{\hat{P}_c \sigma}{R_B \Delta \rho g} \quad (4.9)$$

Table 4.3 gives the results for pancake bubble heights from Eq. (4.9) using the maximum capillary entry pressure from experimental studies shown in Table 4.2 and also using the maximum theoretical capillary entry pressure for hexagonal close-packed spheres. The fluid and sRF resin properties are given in Table 3.2 for each combination of fluid and sRF resin form covered in Table 4.3. The results show that ambient temperature water with sRF resin in the H⁺ form gives the largest pancake bubble for the various fluid / resin pairs. Using the highest experimental literature result for capillary entry pressure, rather than the maximum theoretical value that is overly conservative, the largest pancake bubble is estimated to be 24.2 cm for the ambient water / H⁺-form resin case. For the Section 5.0 calculations of the maximum amount of retained gas under Case 3 conditions, a 30.0 cm (0.3 m) pancake bubble is used as a single bounding height for all fluid / resin conditions. This value exceeds the highest estimated bubble height of 24.2 cm, by about 25% to account for the potential that sRF beads might have a normalized capillary entry pressure that exceeds the largest experimental value found in the literature. While the maximum theoretical value for hexagonal close packing exceeds the selected 30.0 cm bounding value, this theoretical value assumes perfect hexagonal packing, which is very unlikely as shown by the experimental data summarized in Table 4.2 always being about half or less of the theoretical limit. For these reasons, 30.0 cm is used as the bounding pancake bubble height when held by the pore throats of a settled sRF resin bed.

Table 4.3. Pancake Bubble Height Based on Capillary Entry Pressure of the sRF Resin for Different Liquid/sRF Resin Systems

Fluid / sRF Resin Form	<i>h</i> (cm)	
	Highest Value based on Experimental Literature	Maximum Theoretical (Hexagonal Close-Packed)
Ambient Water / Na ⁺	22.7	43.2
Ambient Water / H ⁺	24.2	46.0
Nominal LAW / Na ⁺	21.0	40.0
High-Limit LAW / Na ⁺	22.2	42.1
Bounding Value for Maximum Gas Volume Estimates (Section 5.0)	30.0 ^(a)	

(a) This value exceeds the highest estimated bubble height of 24.2 cm by about 25% to account for the potential that sRF beads might have a normalized capillary entry pressure that exceeds the largest experimental value found in the literature for uniform spherical beads (see Table 4.2). The maximum theoretical value for hexagonal-close-packed beads exceeds the selected 30.0 cm bounding value, but this theoretical value assumes a perfect hexagonal-packed bed, which is very unlikely as demonstrated by the experimental data summarized in Table 4.2 being about half or less of the theoretical limit. For these reasons, 30.0 cm is used as the bounding pancake bubble height when held by the pore throats of a settled sRF resin bed.

5.0 Potential Retained Gas Volume in sRF Resin Bed Released to Break Tank

In this section, the potential retained gas volumes for the three different gas retention cases described in Section 1.1 are calculated. For each of these cases, three sets of liquid and equilibrated resin bead density conditions are evaluated and two gas bubble retention mechanisms within the sRF resin bed are analyzed. Section 5.1 summarizes the calculation method and Section 5.2 provides the results.

5.1 Calculation Method

As described for the three cases in Section 1.1, gas can be retained in the IX column during no-flow conditions both in the resin bed and under the bed or screen (see Section 4.0). This section presents the method for calculating the retained gas volume in the resin bed along with the approach for determining the volume of gas upon release into a break tank headspace.

5.1.1 Resin Bed Retained Gas Volume

As described by Meyer et al. (1997), a sediment bed under a supernatant liquid layer can retain gas until the gas volume renders the bed buoyant in the liquid above it. This limit is used herein to estimate the maximum potential retained gas volume in a bed of sRF resin contained in an IX column. The gas fraction at this neutral buoyant condition, i.e., the volume of gas per the total bed volume (solid, liquid, and gas volume), can be defined by the phase densities and concentrations. For Hanford waste sediment, the neutral buoyant gas fraction is defined in Yarbrough 2013 as

$$\alpha_{NB} = 1 - \frac{\rho_L}{\rho_S} \quad (5.1)$$

where ρ_L is the liquid layer density.¹ The gas-free sediment layer density, ρ_S , herein representing the sRF resin bed, is determined from conservation of mass of the resin beads and liquid matrix by

$$\rho_S = \rho_P(1 - \phi_b) + \rho_L\phi_b \quad (5.2)$$

where ρ_P is the resin bead (particle) density and ϕ_b is the bed porosity. Eq. (5.1) results from a force balance at neutral buoyancy when the gas mass is neglected. Specific to this expression for the neutral buoyant gas fraction is the assumption that the gas bubbles are particle-displacing; an initially degassed bed will increase in volume equal to the volume of gas retained in situ. For liquid-displacing bubbles retained in the resin bed, the total bed volume remains constant at the degassed bed volume but the supernatant liquid volume is increased by the in situ gas volume. In this case, again neglecting the gas mass in the force balance at buoyancy, the neutral buoyant gas fraction can be written as

¹ This definition differs from the critical gas fraction for buoyancy presented in Meyer et al. 1997 as there is no term describing the additional buoyancy required to overcome the bed's yield stress in shear, a phenomenon that is specific to some portion of the bed becoming buoyant and releasing from the surrounding bed material. For the resin bed of packed spheres in the IX column, there is no or extremely limited yield stress from bead-to-bead cohesion (i.e., frictional forces dominate), and the entire bed is considered for buoyancy calculations.

$$\alpha_{NB,LD} = \frac{\rho_P}{\rho_L} (1 - \phi_b) + \phi_b - 1 \quad (5.3)$$

The in situ gas volume is simply the neutral buoyant gas fraction, from either Eq. (5.1) or Eq. (5.3), multiplied by the volume of the gas-containing resin bed. For Eq. (5.1), the volume of the resin bed is increased, while it is constant for Eq. (5.3). The resultant gas volume, which is assumed to be uniformly distributed in the bed volumetrically, can be expressed in terms of moles through the ideal gas law. For these calculations, the gas pressure is a function of its location, as discussed in Section 5.1.3, and a temperature of 20 °C is used (lower temperature results in a larger number of moles for a given volume). From Table 3.2, the density of the Na⁺-form sRF resin beads in water is greater than that of the H⁺ form in water. With a larger resin bead density in the same liquid, the neutral buoyant gas fraction given by either Eq. (5.1) or Eq. (5.3) is increased, thereby increasing the retained gas volume. The Na⁺-form, rather than the H⁺-form, bead and liquid densities for the resin in water system are therefore used in obtaining results below for estimates of the maximum potential retained gas volumes. Such estimates are also obtained for the Na⁺-form resin / nominal LAW simulant and Na⁺-form resin / high-limit LAW simulant pairs using the physical properties summarized in Table 3.2.

5.1.2 Large Bubble Retained Gas Volume

Cases 1 and 3 both have additional gas volumes in pancake bubbles, and Case 2 has a gas volume below the bed equivalent to the neutral buoyant gas volume of the resin bed. The volumes of gas retained in the Case 1 and Case 3 pancake bubbles, either by the screen or the resin bed itself, are determined using the bounding bubble heights developed in Section 4.0. As shown there, the calculated bubble heights are different for bubbles retained by the sRF resin bed and the Johnson screen and also vary with the resin/liquid composition and properties. However, single bounding values were selected and applied for all resin/liquid pairs: 0.1 m for the pancake bubble retained by the screen (Case 1) and 0.3 m for the pancake bubble retained by the resin bed (Case 3). In hypothetical Case 2, where the gas retained in the resin bed is assumed to be relocated to below the bottom screen for determining hydrostatic pressure on the gas, the gas volume is a function of the neutral buoyant gas fraction of the resin bed, which varies with the resin bead and liquid properties according to Eq. (5.1) with Eq. (5.2) or Eq. (5.3). The pancake bubbles in Cases 1 and 3 and the gas volume below the resin bed in Case 2 are assumed to be right circular cylinders spanning the IX column diameter.

5.1.3 Release Volume into Break Tank

As described in Section 1.0, release of the retained gas volume into a break tank headspace is of concern. Therefore, the in situ gas volumes are corrected to headspace volume using the ideal gas law assuming no temperature change between the in situ and headspace conditions. For the gas retained within the resin bed, the pressure at which the gas is assumed to be stored is taken as the hydrostatic pressure at half the resin bed depth, or

$$P_{gas} = P_A + \rho_L g \left(H_L + \frac{H_b}{2} \right) \quad (5.4)$$

where P_A is atmospheric pressure (taken as 101,325 Pa) and H_L and H_b are the supernatant liquid layer and sRF resin bed heights, respectively. As noted in Section 5.1.1, the resin bed height varies with the assumption made for the mechanism of gas bubble retention in the bed, i.e., particle-displacing or liquid-displacing bubbles. The assumptions of hydrostatic head and half-bed depth follow the approach used for flammable gas hazard evaluation in Hanford tank farms waste as described in Yarbrough 2013. A uniform gas fraction profile with sediment depth is a reasonable assumption for the porous resin bed, in which case the entire bed would be buoyant at the same time and the Yarbrough (2013) approach is appropriate. (See Wells et al. 2002 for a discussion of gas fraction profile in tank waste and buoyant depth.) The retained gas pressure in the pancake bubbles for Cases 1 and 3, as well as in the equivalent gas volume of Case 2, is taken as that given by Eq. (5.4), except the full resin bed depth is used.

5.2 Results

The calculated as-retained and as-released gas volumes and the corresponding moles of gas for Cases 1 through 3 are provided in Table 5.1 for neutral buoyant gas fraction with particle-displacing bubbles in the resin bed and in Table 5.2 for neutral buoyant gas fraction with liquid-displacing bubbles in the resin bed. The equivalent break tank volumes at 1 atm pressure are determined using 100% release of the gas volumes retained in the resin bed and below the screen. As noted previously and summarized in the tables, each of the three scenarios is assessed for three Na⁺-form sRF resin/liquid combinations. The tables also show the neutral buoyant gas fractions in the “Resin Bed” cells of the “Gas Location” columns. For Cases 1 and 3 that have pancake bubbles below the screen, Table 5.1 and Table 5.2 give the heights of the idealized pancake bubbles in a cylindrical IX column (not a cone-shaped column bottom as shown in Figure 1.1) that give the noted volumes of retained gas under the screen. For Case 2, as noted in Section 5.1.2, there is no defined pancake bubble and, therefore, no height of gas under the screen is shown in Table 5.1 and Table 5.2. The gas volume “Under screen” in the tables for Case 2 is equivalent to the gas retained in the resin bed at neutral buoyancy that has been hypothetically relocated to the bottom of the sRF resin bed to maximize the hydrostatic pressure.

As discussed in Section 1.1, Case 3 is the worst-case scenario. This is substantiated by the results in Table 5.1 and Table 5.2 that show Case 3 gives the largest break tank gas volume. For each case, the highest break tank gas volumes are achieved with water, followed by nominal LAW simulant, then by the bounding LAW simulant as the liquid in equilibrium with the resin in the IX column. Further, the largest gas volumes in the break tank are achieved using the neutral buoyant gas fraction with liquid-displacing bubbles, which are the results in Table 5.2, rather than particle-displacing bubbles (Table 5.1). For all the cases and different fluids, Case 3 with water gives the maximum calculated amount of gas in the break tank headspace, which is a volume of 0.521 m³ at 1 atm pressure and 20 °C that corresponds to 21.6 moles retained in the column at 20 °C (Table 5.2).

Table 5.1. Results for Cases 1 through 3, Particle-Displacing Bubbles

Liquid in Ion Exchange Column	Gas Location (α_{NB})	Case 1			Case 2		Case 3		
		moles	m ³	Height m	moles	m ³	moles	m ³	Height m
Water	Resin bed (0.126)	7.94	0.165	N/A	N/A	N/A	7.94	0.165	N/A
	Under screen	4.55	0.0894	0.1	8.30	0.165	13.6	0.268	0.3
	Equivalent break tank volume	12.5	0.300	N/A	8.30	0.200	21.6	0.519	N/A
Nominal LAW	Resin bed (0.066)	3.98	0.0808	N/A	N/A	N/A	3.98	0.0808	N/A
	Under screen	4.70	0.0894	0.1	4.22	0.0808	14.1	0.268	0.3
	Equivalent break tank volume	8.68	0.209	N/A	4.22	0.101	18.1	0.435	N/A
Bounding LAW	Resin bed (0.042)	2.51	0.0504	N/A	N/A	N/A	2.51	0.0504	N/A
	Under screen	4.78	0.0894	0.1	2.68	0.0504	14.3	0.268	0.3
	Equivalent break tank volume	7.29	0.175	N/A	2.68	0.0644	16.8	0.405	N/A

N/A = not applicable

Table 5.2. Results for Cases 1 through 3, Liquid-Displacing Bubbles

Liquid in Ion Exchange Column	Gas Location ($\alpha_{NB,LD}$)	Case 1			Case 2		Case 3		
		moles	m ³	Height m	moles	m ³	moles	m ³	Height m
Water	Resin bed (0.145)	8.00	0.165	N/A	N/A	N/A	8.00	0.165	N/A
	Under screen	4.55	0.0894	0.1	8.30	0.165	13.6	0.268	0.3
	Equivalent break tank volume	12.5	0.302	N/A	8.30	0.200	21.6	0.521	N/A
Nominal LAW	Resin bed (0.071)	4.00	0.0808	N/A	N/A	N/A	4.00	0.0808	N/A
	Under screen	4.70	0.0894	0.1	4.22	0.0808	14.1	0.268	0.3
	Equivalent break tank volume	8.70	0.209	N/A	4.22	0.101	18.1	0.435	N/A
Bounding LAW	Resin bed (0.044)	2.52	0.0504	N/A	N/A	N/A	2.52	0.0504	N/A
	Under screen	4.78	0.0894	0.1	2.68	0.0504	14.3	0.268	0.3
	Equivalent break tank volume	7.30	0.176	N/A	2.68	0.0644	16.9	0.405	N/A

N/A = not applicable

The volume of gas released into the break tank is dependent on the liquid head above the retained gas as given by Eq. (5.4). Design details of the IX column, piping above the column, and location/elevation of the break tank are not yet available, so the maximum liquid column height is currently unknown. Alternatively, the release volume at atmospheric pressure for the maximum gas volume scenario (Case 3 with water and liquid-displacing bubbles) can be determined for a range of liquid column heights above the Johnson screen to allow maximum release volume estimates for a range of potential configurations. Figure 5.1 gives the results for release volume as a function of the initial (pre-gas-retention) height of the liquid column above the Johnson screen. Also included for comparison are the results for Case 1 with water and liquid-displacing bubbles. The initial (lowest) values for Cases 1 and 3 in Figure 5.1 are the respective values from Table 5.2 with an initial (pre-gas-retention) water column height of 2.13 m (84 in.). The nominally 50% increase in liquid column height results in an approximately 9% increase in the gas release volume.

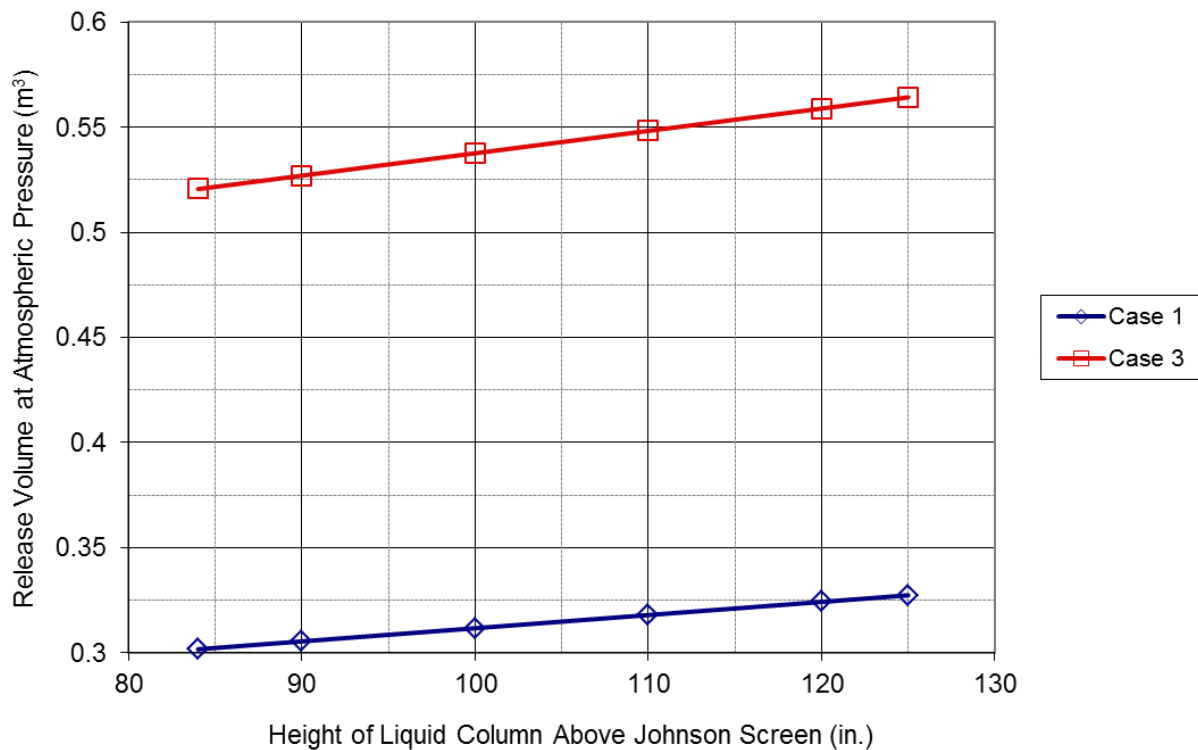


Figure 5.1. Release volume for Table 5.2 limiting cases as a function of height of liquid column above Johnson screen.

6.0 Conclusions

Three cases were considered for the location and quantity of retained gas, and for each case, results were obtained for two different gas retention mechanisms and three different fluid / sRF resin pairs. These cases and conditions were selected to provide bounding (maximum) estimates of the gas volume released. Based on an analysis of these cases, the following conclusions were reached:

- The largest released gas volume occurs with water / Na⁺-form sRF resin in the column in comparison to a nominal LAW or a bounding high-density LAW as the liquid in equilibrium with sRF resin.
- The largest released gas volume occurs using the neutral buoyant gas fraction determined with gas retained within the resin bed in liquid-displacing bubbles rather than by the alternate particle-displacing bubble gas retention mechanism.
- The largest released gas volume occurs with a bounding 30 cm (0.3 m) high pancake bubble retained beneath the resin bed (and bottom screen), resulting from capillary entry pressure restrictions at pore throats of the packed spherical resin beads.
- The maximum calculated volume of released gas is 0.521 m³ at 1 atm pressure and 20 °C that corresponds to 21.6 moles retained in the column at 20 °C, assuming a pre-gas-retention liquid depth of 2.13 m (84 in.) above the bottom screen.
- The volume of gas released increases by approximately 9% for a nominally 50% increase in pre-gas-retention liquid depth in the system from 2.13 m (84 in.) to 3.18 m (125 in.).

7.0 References

- Aguilar F. 2016. *Test Specification for the Low-Activity Waste Pretreatment System Full-Scale Ion Exchange Column Test and Engineering-Scale Integrated Test (Project T5L01)*. RPP-RPT-58683, Rev. 3, Washington River Protection Solutions LLC, Richland, WA.
- Ansolabehere AA. 2016. *Project T5L01 Low Activity Waste Pretreatment System Specification*. RPP-SPEC-56967, Rev. 6, Washington River Protection Solutions LLC, Richland, WA.
- Colburn HA, SA Bryan, DM Camaioni, and LA Mahoney. 2017. *Gas Generation Testing of Spherical Resorcinol-Formaldehyde (sRF) Resin*. PNNL-26869 (RPT-LPIST-002), Rev. 0, Pacific Northwest National Laboratory, Richland, WA. (to be published)
- CRC. 2005. *Handbook of Chemistry and Physics*, 86th edition, DR Lide (ed.). CRC Press, Taylor & Francis Group, Boca Raton, FL.
- Dullien FAL. 1979. *Porous Media: Fluid Transport and Pore Structure*, 1st edition. Academic Press, Inc., New York, NY.
- Dullien FAL. 1992. *Porous Media: Fluid Transport and Pore Structure*, 2nd edition. Academic Press, Inc., San Diego, CA.
- Falls AH, GJ Hirasaki, TW Patzek, PA Gauglitz, DD Miller and J Ratulowski. 1988. "Development of a Mechanistic Foam Simulator: The Population Balance and Generation by Snap-Off." *Soc. Petr. Eng. Reservoir Eng.* 3(1988):884-892.
- Flint AL and LE Flint. 2002. *Particle Density*. Methods of Soil Analysis, Part 4: Physical Methods, JH Dane, GC Topp, and GS Campbell (eds.), SSSA Book Series No. 5, pp. 229-240. SSSA, Madison, WI.
- Gauglitz PA, WC Buchmiller, SG Probert, AT Owen, and FJ Brockman. 2012. *Strong-Sludge Gas Retention and Release Mechanisms in Clay Simulants*. PNNL-21167 (EMSP-RPT-013), Rev. 0, Pacific Northwest National Laboratory, Richland, WA.
- Kruyer S. 1958. "The Penetration of Mercury and Capillary Condensation in Packed Spheres." *Trans. Faraday Soc.* 54(1958):1758-1767.
- Meyer PA, ME Brewster, SA Bryan, G Chen, LR Pederson, CW Stewart, and G Terrones. 1997. *Gas Retention and Release Behavior in Hanford Double-Shell Waste Tanks*. PNNL-11536, Rev. 1, Pacific Northwest National Laboratory, Richland, WA.
- Morrow NR and CC Harris. 1965. "Capillary Equilibrium in Porous Materials." *Soc. Petr. Eng. J.* 5(1965):15-24.
- Norton JD and LR Pederson. 1994. *Ammonia in Simulated Hanford Double-Shell Tank Wastes: Solubility and Effects on Surface Tension*. PNL-10173, Pacific Northwest Laboratory, Richland, WA.

NQA-1-2000, *Quality Assurance Requirements for Nuclear Facility Applications*. American Society of Mechanical Engineers, New York, NY.

NQA-1-2008, *Quality Assurance Requirements for Nuclear Facility Applications*. American Society of Mechanical Engineers, New York, NY.

NQA-1a-2009, *Addenda to ASME NQA-1-2008*. American Society of Mechanical Engineers, New York, NY.

Schonewill PP, PA Gauglitz, RW Shimskey, KM Denslow, MR Powell, GK Boeringa, JR Bontha, NK Karri, LS Fifield, DN Tran, SA Sande, DJ Heldebrant, JE Meacham, DB Smet, WE Bryan, and RB Calmus. 2014. *Evaluation of Gas Retention in Waste Simulants: Tall Column Experiments*. PNNL-23340 (DSGREP-RPT-005), Rev. 0, Pacific Northwest National Laboratory, Richland, WA.

Wells BE, JM Cuta, SA Hartley, LA Mahoney, PA Meyer, and CW Stewart. 2002. *Analysis of Induced Gas Releases During Retrieval of Hanford Double-Shell Tank Waste*. PNNL-13782 Rev. 1, Pacific Northwest National Laboratory, Richland, WA.

Yarbrough RJ. 2013. *Methodology and Calculations for the Assignment of Waste Groups for the Large Underground Waste Storage Tanks at the Hanford Site*. RPP-10006, Rev. 11, Washington River Protection Solutions LLC, Richland, WA.

Distribution*

Washington River Protection Solutions

KE Ard
SM Kim
MR Landon
JG Reynolds
RM Russell
TE Sackett
WRPS Documents – TOCVND@rl.gov
LAWPS Document – LAWPSVENDOR@rl.gov

Savannah River National Laboratory

DT Herman

DOE – Office of River Protection

SC Smith

Pacific Northwest National Laboratory

CLH Bottenus
PA Gauglitz
DT Linn
LA Mahoney
SD Rassat
PP Schonewill
BE Wells
Project File
Information Release (pdf)

*All distribution will be made electronically.



Pacific Northwest
NATIONAL LABORATORY

*Proudly Operated by **Battelle** Since 1965*

902 Battelle Boulevard
P.O. Box 999
Richland, WA 99352
1-888-375-PNNL (7665)

U.S. DEPARTMENT OF
ENERGY

www.pnnl.gov